JOURNAL OF VIROLOGY, Oct. 2011, p. 9667–9679 Vol. 85, No. 19
0022-538X/11/$12.00 doi:10.1128/JVI.05314-11

A Functional Role for TorsinA in Herpes Simplex Virus 1 Nuclear Egress▽

Martina Maric,[1] Jianqiang Shao,[2] Randi J. Ryan,[1] Chun-Shu Wong,[3] Pedro Gonzalez-Alegre,[4] and Richard J. Roller[1]*

Department of Microbiology, University of Iowa, Iowa City, Iowa 52242[1]; Central Microscopy Research Facilities, University of Iowa, Iowa City, Iowa 52242[2]; Program in Immunology, University of Michigan, Ann Arbor, Michigan 48109[3]; and Department of Neurology, University of Iowa, Iowa City, Iowa 52242[4]

Received 6 June 2011/Accepted 8 July 2011

Herpes simplex virus 1 (HSV-1) capsids leave the nucleus by a process of envelopment and de-envelopment at the nuclear envelope (NE) that is accompanied by structural alterations of the NE. As capsids translocate across the NE, transient primary enveloped virions form in the perinuclear space. Here, we provide evidence that torsinA (TA), a ubiquitously expressed ATPase, has a role in HSV-1 nuclear egress. TA resides within the lumen of the endoplasmic reticulum (ER)/NE and functions in maintaining normal NE architecture. We show that perturbation of TA normal function by overexpressing torsinA wild type (TAwt) inhibits HSV-1 production. Ultrastructural analysis of infected cells overexpressing TAwt revealed reduced levels of surface virions in addition to accumulation of novel, double-membrane structures called virus-like vesicles (VLVs). Although mainly found in the cytoplasm, VLVs resemble primary virions in their size, by the appearance of the inner membrane, and by the presence of pUL34, a structural component of primary virions. Collectively, our data suggest a model in which interference of TA normal function by overexpression impairs de-envelopment of the primary virions leading to their accumulation in a cytoplasmic membrane compartment. This implies novel functions for TA at the NE.

Following capsid assembly and DNA packaging, herpesvirus DNA-containing capsids in the nucleus translocate through the nuclear envelope (NE) into the cytoplasm by envelopment at the inner nuclear membrane (INM), followed rapidly by de-envelopment at the outer nuclear membrane (ONM). Between envelopment and de-envelopment, enveloped capsids called primary virions reside briefly in the perinuclear space that is contiguous with the lumen of the endoplasmic reticulum (ER) (reviewed in reference 34).

Nuclear envelopment requires expression of the viral pUL31 and pUL34 (7, 14, 27, 44, 48). These proteins form a complex that is targeted to the NE and anchored in the membrane by the transmembrane domain of pUL34 (44, 45, 64, 65). The pUL34/pUL31 complex coordinates multiple events in nuclear egress, including disruption of the nuclear lamina, selection of DNA-containing capsids for envelopment, budding of capsids into the INM, and de-envelopment and release of capsids at the ONM (2, 30, 38, 43, 46, 53). pUL31 and pUL34 are incorporated into the perinuclear virion and are ordinarily lost from the egressing capsid upon de-envelopment at the ONM (14, 27, 31, 42, 45). Thus, they are not associated with cytoplasmic egress intermediates or with the mature virion that is released from the cell.

De-envelopment may be inhibited and/or delayed by mutations in several herpes simplex virus (HSV) gene products. Mutations that eliminate either the expression or kinase activity of pUS3 result in accumulation of primary virions in the perinuclear space. During infection with these mutants, the perinuclear space expands by bulging into the nucleoplasm, perhaps because the exaggerated disruption of the nuclear lamina associated with loss of pUS3 function makes this the path of least resistance (2, 28, 36–38, 45, 49). A de-envelopment defect is also observed in cells infected with recombinant mutants of HSV-1 that fail to express both of the envelope glycoproteins gB and gH (13).

Infection with HSV-1 alters the morphology and structure of the NE. The nucleus expands and changes shape. In addition, redistribution of nuclear lamina proteins is observed, most likely due to phosphorylation-mediated loss of protein-protein interactions (2, 30, 35, 36, 43, 49, 50, 53, 54). In addition to these changes, formation of perinuclear primary virions is likely to be accompanied by alteration of interactions that maintain spacing between the INM and ONM.

The product of the *DYT1* (*TOR1A*) gene, torsinA (TA), is important for maintaining NE architecture and possibly spacing of the nuclear membranes. TA is an essential protein in mice and is one of four members of the torsin protein family in mammals, which is part of the large and diverse AAA^+ (ATPases associated with diverse cellular activities) superfamily of ATPases (41, 62). Biochemical and localization studies showed that TA is a fully translocated glycoprotein, predominantly found in the ER lumen and the NE (5, 15). Mutation in the *DYT1* gene that leads to a loss of a single glutamic acid residue, Glu^{302} or Glu^{303}, near the C terminus of TA is associated with dominantly inherited early-onset torsion dystonia (21, 62). This movement disorder, characterized by involuntary sustained muscle contraction causing twisting movements and abnormal posture, is believed to be a nuclear envelopathy whose pathogenesis is correlated with defects in TA function specifically in neurons (19, 63).

* Corresponding author. Mailing address: Department of Microbiology, The University of Iowa, 3-432 Bowen Science Building, Iowa City, IA 52242. Phone: (319) 335-9958. Fax: (319) 335-9006. E-mail: richard-roller@uiowa.edu.

▽ Published ahead of print on 20 July 2011.

The biological significance of TA is largely unknown. Several functions, including a role as a molecular chaperone and a homeostatic regulator of an induced ER stress response, have been suggested for TA but are not well understood (3, 4, 8, 24, 33). In addition, neurons from mouse *DYT1* dystonia models showed disruption of the perinuclear space, thus pointing to NE as an important site of TA action. Neuronal cells from *DYT1* knockout and dystonia mutant TA (TAmut) knock-in mice showed enlarged perinuclear space associated with blebbing of the INM (19, 26). A similar function in maintaining nuclear architecture was also shown for torsinB (TB), which is 65% identical to TA, but not for two other, less closely related torsin family members (21, 26). Interestingly, disruption of the NE was also observed when cells expressed abnormally high levels of torsins (22, 26, 39). In neurons overexpressing wild-type TA (TAwt), perinuclear blebs formed that appeared indistinguishable from the blebs seen in neurons from TA knockout mice. A similar phenotype at the NE was also observed when TB was overexpressed (26). These data strongly suggest that overexpression of TAwt or TB interferes with their normal function in maintaining normal NE architecture.

The critical role played by torsin family members in maintenance of proper NE functions suggests that these proteins may play an important role in nuclear egress of herpesviruses. The perturbation of TA normal function at the NE by overexpression provides a powerful tool for testing the significance of normal TA function in HSV infection in a variety of cell types. Here, we demonstrate (i) that TAwt overexpression impairs HSV-1 production without affecting accumulation of virus proteins or capsid assembly, (ii) that TAwt overexpression leads to formation of novel structures called virus-like vesicles (VLVs), which are primary virions that accumulate inside cytoplasmic membranes, presumably the ER, and (iii) that TA colocalizes with cytoplasmic primary virions.

MATERIALS AND METHODS

Cells, viruses, and chemicals. PC6-3 cells that stably express torsinA wild type (PC6-3TAwt) or dystonia mutant torsinA (PC6-3TAmut) were described previously (17). Cells were grown on rat collagen (BD Biosciences)-coated dishes in RPMI 1640 medium supplemented with 10% equine serum, 5% fetal bovine serum (FBS), 100 μg/ml hygromycin, 100 U/ml penicillin, and 100 μg/ml streptomycin (Pen-Strep). For TA induction, 1.5 μg/ml doxycycline (DOX) (Sigma) was added to the growth medium. Vero cells were maintained as described previously (48). Human embryonic kidney (HEK) 293T cells were grown in Dulbecco's modified Eagle's medium (DMEM) supplemented with 10% FBS and Pen-Strep. The properties of wild-type HSV-1 strain F [HSV-1(F)] and HSV-1(F) bacterial artificial chromosome (BAC) genomes carrying a UL34 deletion (UL34-null) were described previously (46, 56). A BAC expressing a monomeric red fluorescent protein (mRFP) fused to VP26 (rHSVBAC35R) was kindly provided by Cornel Fraefel (University of Zurich, Switzerland) (11). The VP5-null virus was a generous gift of Prashant Desai (12) and was propagated on VP5-expressing Vero cells.

Plasmids. The enhanced green fluorescent protein (EGFP) expression vector (pEGFP-C1) was obtained from Clontech. GFP-tagged wild-type TA (GFP-TAwt) and wild-type torsinB (GFP-TB) constructs were generously provided by Phyllis Hanson, Washington University School of Medicine, St. Louis, MO (39). Red fluorescent protein with an ER retention signal (RFP-KDEL) was a kind gift of Thomas Rutkowski, University of Iowa.

Viral growth assay. For single-step growth analysis, PC6-3 cells were seeded in 12-well plates coated with rat collagen and were mock or DOX treated for 14 h. After the TA induction, cells were infected with HSV-1(F) at a multiplicity of infection (MOI) of 5, and residual virus was removed or inactivated with a low-pH buffer wash at 1 h postinfection (hpi). Cultures were maintained in normal rat growth medium with or without DOX. At various time points, the cultures were frozen and thawed to lyse the cells and briefly sonicated, and titers of infectious virus were determined by plaque assay on Vero cells as described previously (48). Statistical significance was determined using a two-tailed, unpaired (two-sample) Student's *t* test.

TEM. Confluent T-25 flasks of PC6-3TAwt or PC6-3TAmut cells were mock or DOX treated for 16 h. After the treatment, cells were infected with mock, HSV-1(F), or VP5-null virus at an MOI of 10. At 20 hpi cells were fixed, processed, and analyzed using a JEOL 1230 transmission electron microscope (TEM) as described previously (46).

Cryo-ultramicrotomy and immunolabeling. Confluent T-25 flasks of mock- or DOX-treated PC6-3TAwt cells were infected with HSV-1(F) at an MOI of 10 for 20 h. For cryo-ultramicrotomy, cells were fixed in 4% paraformaldehyde plus 0.2% glutaraldehyde in phosphate-buffered saline (PBS), scraped from the flask, and then embedded in 10% gelatin. After the gelatin had solidified, small blocks were cut and infused with 2.3 M sucrose in PBS. The samples were then frozen in liquid nitrogen and ultrathin (60 nm) cryosections were prepared (Leica EM UC6 ultramicrotome; Bannockburn, IL) and deposited onto a 300-mesh Ni grid coated with Formvar plus carbon. For pUL34 detection, cryosections were incubated with chicken polyclonal antibody anti-pUL34 overnight at 4°C, followed by a 30-min room temperature incubation with 6-nm gold-conjugated goat anti-chicken IgG (Electron Microscopy Sciences/Aurion, Hatfield, PA). Antibodies were diluted in 0.1% BSA-c (where BSA is bovine serum albumin; Electron Microscopy Sciences/Aurion, Hatfield, PA) in PBS, and the same buffer was also used for washing steps. After labeling, grids were poststained with a mixture of 2% methylcellulose and 0.3% uranyl acetate and analyzed with a JEOL 1230 TEM.

Western blot analysis. To determine the accumulation of TA and virus proteins, PC6-3 cells were induced with mock treatment or DOX for 14 h and then infected with HSV-1(F) at an MOI of 5. At 12 hpi cultures were scraped, washed one time with PBS, and pelleted at low speed. Cells were then lysed in 1× SDS sample buffer (39001; Thermo Scientific) with added β-mercaptoethanol (Sigma) and boiled for 10 min. Cell lysates were briefly sonicated, and total protein concentration was determined using a Bio-Rad detergent-compatible (DC) protein assay (Bio-Rad Laboratories). Equal amounts of protein were loaded on SDS-PAGE gels, electrically transferred to a nitrocellulose sheet, and probed with the following antibodies and dilutions: rabbit polyclonal anti-human TA (1:1,000) (17), mouse monoclonal anti-VP5/H1.4 (1:1,000) (Meridian, Life Science), mouse monoclonal anti-pUS11 (1:1,000) (47), chicken polyclonal antibody anti-pUL34 (1:1,000) (44), mouse monoclonal anti-gC (1:1,000) (H1A022; Virusys), mouse monoclonal anti-gD/DL6 (1:5,000), mouse anti-gB/SS55 (1:500), mouse anti-gH/H12 (1:500), and mouse gL/L4 (1:500). Antibodies DL6, SS55, H12, and L4 were kindly provided by Gary H. Cohen and Roselyn J. Eisenberg (University of Pennsylvania). Secondary alkaline phosphatase-conjugated anti-rabbit (A3562; Sigma), anti-mouse (A3562; Sigma), and anti-chicken (AP1001; Aves Lab) antibodies were incubated with the appropriate blot for 30 min.

Indirect IF. For localization studies PC6-3 cell lines were mock or DOX induced for 14 h and then infected with HSV at an MOI of 5. At 16 hpi cells were fixed with 4% formaldehyde in PBS for 10 min, washed once with PBS, and then permeabilized and blocked in the same step by incubation overnight at 4°C in IF buffer (0.5% Triton X-100, 0.5% sodium deoxycholate, 1% bovine serum albumin, 0.05% sodium azide in PBS). The immunofluorescence (IF) buffer was supplemented with 5% goat serum (Sigma) or 10% pooled human gamma globulin (Gammar; Armour Pharmaceutical) when rabbit polyclonal anti-TA antibodies were used. Primary antibodies were diluted in IF buffer as follows: rabbit polyclonal anti-human torsinA (1:800), chicken polyclonal anti-pUL34 (1:1000), and mouse monoclonal anti-LAP2 (1:200) (61100; BD Transduction Laboratories). Secondary antibodies (Invitrogen) were diluted 1:1,000 in IF buffer as follows: Alexa Fluor donkey anti-rabbit IgG, Alexa Fluor goat anti-chicken IgG, and Alexa Fluor goat anti-mouse. A SlowFade antifade kit (Invitrogen) was used to mount coverslips on glass slides. All confocal microscopy work was done with a Zeiss 510 confocal microscope.

HSV-1 growth in HEK 293T cells overexpressing torsins. For HSV-1 growth analysis in HEK 293T cells overexpressing torsins, cells were seeded in a 12-well plate coated with poly-L-lysine (Sigma) and transfected with GFP and GFP-tagged torsin constructs using Lipofectamine 2000 (Invitrogen) according to the manufacturer's instructions. Transfection efficiency was measured by determining GFP-expressing cells via flow cytometry (BD FACSCalibur) 24 h later. Acquired data were analyzed using WinMDI, version 2.8 (Joe Trotter). In only the experiments where all the constructs transfected at least 90% of the cells, cultures were then infected with HSV-1(F) at an MOI of 5, and residual virus was removed or inactivated with a low-pH buffer wash 1 h later. Virus titers were determined at 16 hpi by plaque assay on Vero cells. An unpaired Student's *t* test was used to calculate *P* values.

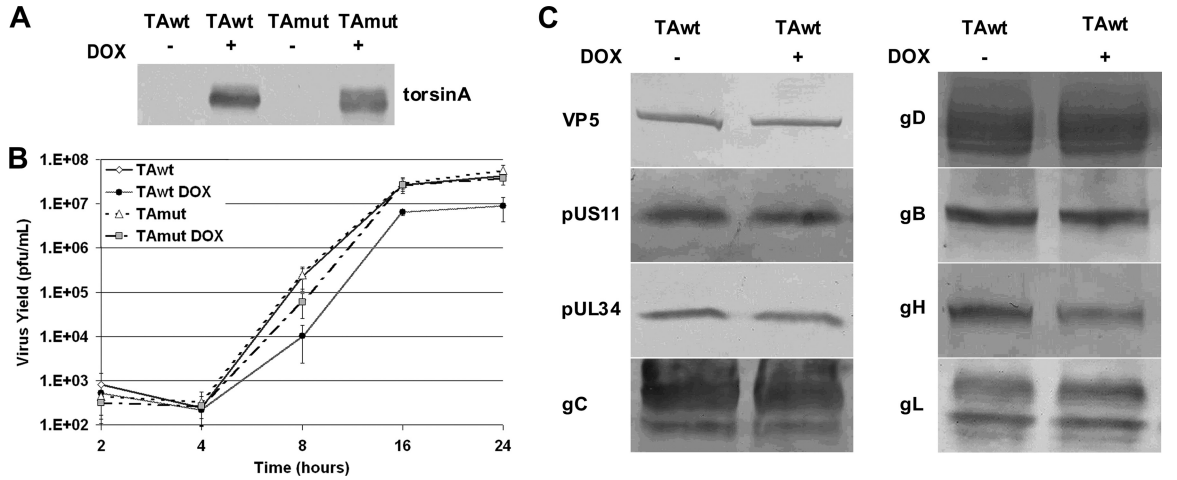

FIG. 1. Overexpression of TAwt inhibits HSV-1 production in rat PC6-3 cells. (A) Expression of TAwt in PC6-3-TAwt and TAmut in PC6-3-TAmut cells. PC6-3-TAwt and PC6-3-TAmut cells were mock or DOX induced for 14 h, infected with HSV-1(F) at 5 PFU/cell for 12 h, and blotted for human TA. (B) Single-step growth curves of HSV-1(F) on PC6-3 cell lines. PC6-3-TAwt and PC6-3-TAmut cells were mock or DOX treated and then infected with HSV-1(F) at an MOI 5. At the indicated time points, virus infectivity of the whole culture was determined on Vero cells. Virus yields are expressed as the number of PFU per milliliter. Each datum point represents the mean of three experiments. (C) Accumulation and processing of HSV-1 gene products in PC6-3-TAwt cells. The experiment is as described in panel A. Western blots were probed with antibodies to proteins indicated on left. The depicted blots are representative of two separate experiments.

RESULTS

TorsinA wild-type overexpression impairs HSV-1 production in rat cells. TA function helps to maintain normal nuclear architecture and, as such, might either enhance or interfere with HSV replication. Thus, it seemed likely that overexpression of either TAwt or TAmut might impair or promote viral replication. To test this, we took advantage of rat PC6-3 clonal cell lines PC6-3TAwt and PC6-3TAmut that express human wild-type and dystonia mutant TA, respectively, under the control of a doxycycline (DOX)-inducible promoter (17, 32). As shown previously, protein levels of the wild-type and mutant TA protein after induction with DOX were similar (data not shown) and were not affected by HSV-1 infection (Fig. 1A), allowing us to interpret phenotypic differences in terms of differences in function rather than differences in expression. The rat endogenous TA is not detected. Single-step growth of HSV-1(F) was measured on PC6-3TAwt and PC6-3TAmut cells that were untreated or that had been induced by exposure to DOX (Fig. 1B). HSV-1 production by uninduced TAwt or TAmut cells is similar. Induction of TAwt resulted in statistically significant inhibition of HSV-1 replication at all times after the eclipse phase (at 8 [$P < 0.037$], 16 [$P < 0.023$], and 24 [$P < 0.007$] hpi), decreasing virus peak titers roughly 5-fold. That this is not simply an overexpression artifact is demonstrated by overexpression of TAmut, which did not significantly affect HSV-1 peak titers.

To determine if TAwt overexpression interferes with early events in the virus life cycle (virus entry, gene expression, and DNA replication), we performed immunoblotting to measure accumulation of HSV-1(F) gene products in uninduced or DOX-induced PC6-3TAwt cells (Fig. 1C). Comparable levels of HSV-1 late (VP5 and pUL34) and true late proteins (pUS11, gC, and gH) accumulate in mock- and DOX-treated cells. These data suggest that inhibition of virus growth is not due to global defects that precede late gene expression and is more likely due to defects in the assembly and egress phase of infection. Since TA is an ER-luminal ATPase possibly acting as a molecular chaperone (3, 4, 24, 33), we investigated the consequence of TA overexpression on processing and localization of viral glycoproteins. Western blot analysis showed no differences in band migration of five tested glycoproteins (gC, gD, gB, gH, and gL) in cells overexpressing TAwt (Fig. 1C), indicating that the posttranslational modification of virus glycoproteins is not grossly affected. In addition, localization studies of gD, gB, gH, and gL using immunofluorescence (IF) showed no torsin-dependent change in localization of any of the tested glycoproteins (data not shown).

TorsinA wild-type overexpression leads to accumulation of virus-like vesicles (VLVs) in the cytoplasm. Alterations in TA protein levels or function were intuitively expected to influence nuclear egress. To test this possibility, DOX-induced or uninduced PC6-3TAwt and PC6-3TAmut cells were mock infected or infected with 10 PFU/cell of HSV-1(F) for 20 h and then examined by transmission electron microscopy (TEM) (Fig. 2). Ultrastructural analysis of uninfected DOX-induced PC6-3TAwt cells revealed large, double-membrane blebs at the NE (Fig. 2A, white arrowhead) in 5 out of 10 cells. These NE abnormalities caused by TAwt overexpression have been reported previously and are very similar to NE blebs observed in neurons from TA-null mice (19, 26). Infection with HSV did not change the frequency of cells that formed NE blebs.

In Fig. 2B a typical section of HSV-1-infected PC6-3TAwt cells with capsids in the nucleus (black arrowhead) and mature virions on the cell surface (white arrowhead) is shown. In addition to numerous capsids (Fig. 2Da) and surface virions (Fig. 2Dd), perinuclear virions (Fig. 2Db) and mature virions in the cytoplasm (Fig. 2Dc) were also occasionally observed (Table 1). In infected cells that had been induced for TAwt overexpression, two striking differences were observed (Fig. 2C). First, about 6-fold fewer mature virions were present at

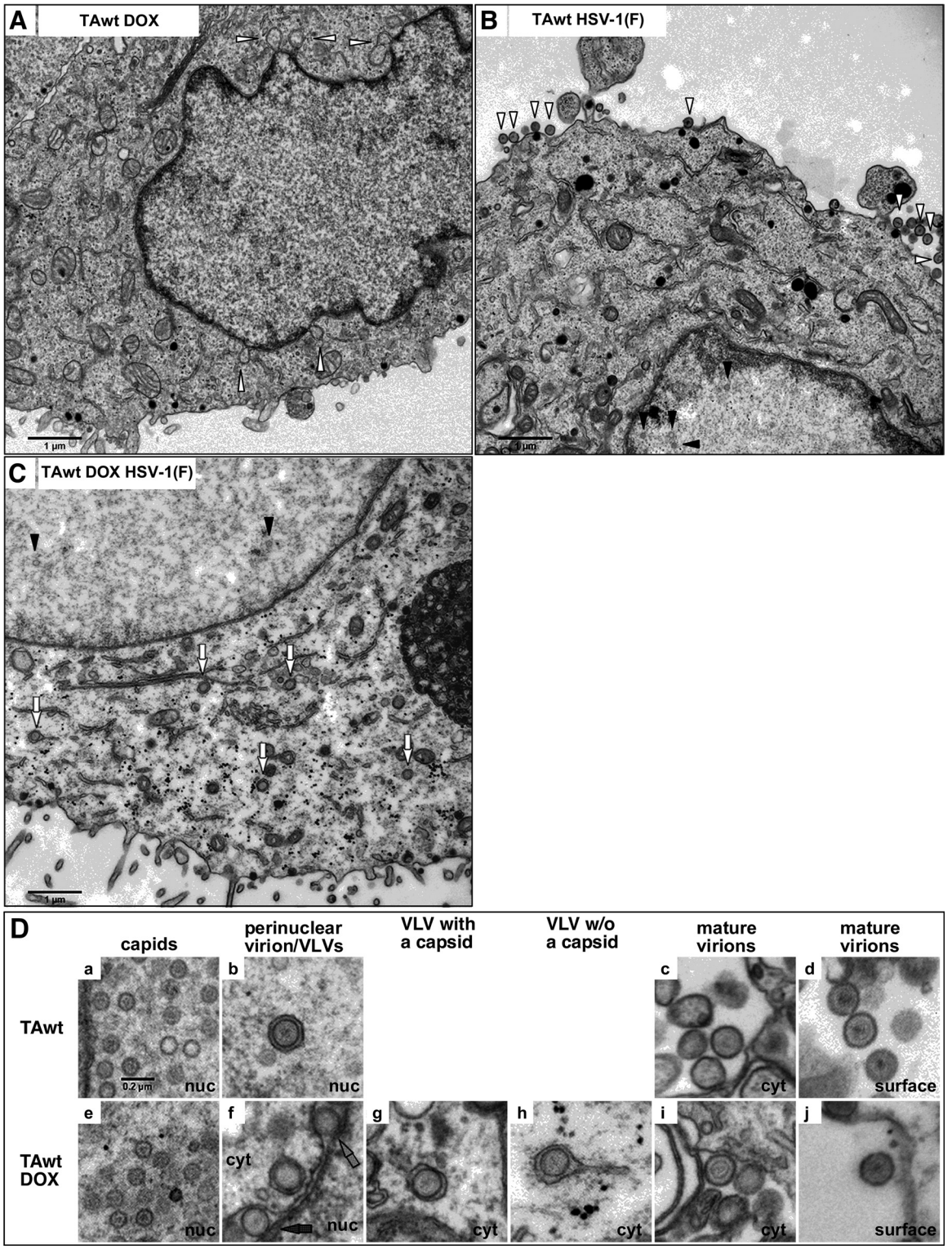

FIG. 2. Ultrastructural analysis of PC6-3TAwt cells. Shown are micrographs of PC6-3-TAwt cells that were mock (B) or DOX treated (A and C) for 16 h and then infected with mock virus (A) or HSV-1(F) (B and C) at an MOI of 10 for 20 h. In panel A, the white arrowheads point to blebs at the NE. Examples of virions at the cell surface (B, white arrowhead), capsids in the nucleus (B and C, black arrowhead), and VLVs (C, white arrow) are indicated. Stages of HSV-1 assembly in mock-induced (a to d) and DOX-induced (e to j) PC6-3TAwt cells are shown in panel D. In frame f, perinuclear VLVs with and without a capsid are highlighted by black and gray arrows, respectively. nuc, nucleus; cyt, cytoplasm. The scale in μm is indicated. All frames in panel D are shown at the same magnification. w/o, without.

TABLE 1. Numbers and percentages of virus particles in HSV-1(F)-infected PC6-3TAwt cells[a]

Cell type	No. (%) of nuclear capsids	No. (%) of perinuclear virions	No. (%) of perinuclear VLVs	No. (%) of cytoplasmic virus particles				No. (%) of surface virions	Total no. (%) of counted particles
				Naked capsids	Mature virions	VLVs without a capsid	VLVs with a capsid		
HSV-1(F)-infected PC6-3TAwt	413 (61.8)	4 (0.6)	3 (0.4)	60 (9.0)	21 (3.1)	0 (0)	0 (0)	167 (25.0)	668 (100)
HSV-1(F)-infected, DOX-treated PC6-3TAwt	447 (64.6)	7 (1.0)	10 (1.4)	70 (10.1)	10 (1.4)	65 (9.4)	56 (8.1)	27 (3.9)	692 (100)

[a] TEM images of 10 randomly selected cells with at least one capsid or margination of chromatin were taken and subsequently counted for virus particles.

the cell surface (Table 1), which is similar to the decrease in virus production observed in single-step growth. Second, novel structures that we named virus-like vesicles (Fig. 2C, white arrows) accumulated in the cytoplasm. We defined VLVs as circular membrane vesicles enclosing a capsid (Fig. 2Df, black arrow, and g) or undefined material (Fig. 2Df, gray arrow, and h) where the membrane had a sharp, electron-dense appearance and the diameter of an HSV virion. VLVs were observed in the perinuclear space (Fig. 2Df, arrows) and/or in the cytoplasm (Fig. 2Dg and h). Cytoplasmic VLVs were enclosed in a second, irregular membrane (Fig. 2Dg and h). VLVs were observed in 9 out of 10 cells examined, and their number varied from 1 to 29 per cell section. In infected rat cells overexpressing TAwt, cytoplasmic VLVs represent the major form (69%) of enveloped membranous virus particles. For comparison, cytoplasmic mature virions in uninduced cells correspond to 11% of total envelope virus particles.

The sharp appearance of the VLV membrane closely resembles the envelope of a primary virion (Fig. 2D, compare b with g and h). Unlike primary virions, however, the vast majority of VLVs were found in the cytoplasm away from the nuclear membrane (Table 1). That cytoplasmic VLVs were surrounded by an additional membrane raised the possibility that VLVs represent mature virions inside transport vesicles that were abnormally accumulating in the cytoplasm. The following comparisons suggested that VLVs did not correspond to mature virions: (i) the envelopes of VLVs lack the characteristic "fuzzy" appearance of mature virion envelopes (Fig. 2D, compare g and h with c, d, i, and j); (ii) VLVs were closely surrounded by an irregular, sometime tubular-shaped membranes while mature virions, on the other hand, were predominantly found inside large and hollow-appearing vesicles (Fig. 2D, compare g and h with c and i); (iii) VLVs were distributed throughout the cytoplasm (Fig. 2C) while mature virions were predominately associated with a cellular compartment composed of distinct hollow membranous stacks (data not shown). In summary, the primary virion-like envelope of VLVs and their distinctiveness from mature virions strongly suggested that VLVs were a product of primary rather than secondary envelopment.

VLVs were not observed following infection of uninduced or DOX-induced PC6-3TAmut cells in 10 randomly examined cells, indicating that production of VLVs in these cells specifically requires overexpression of TAwt.

Since obvious capsids were not visible in more than half of VLVs (Table 1), we asked if the formation of VLVs could be triggered in the absence of capsid envelopment by examining uninduced or DOX-induced PC6-3TAwt cells infected with VP5-null virus. In 10 randomly examined cells, we did not observe a VLV in VP5-null virus-infected cells overexpressing TAwt, indicating that VLV formation is capsid dependent.

Overexpression of torsinA wild type redistributes pUL34 into cytoplasmic puncta that colocalize with a capsid protein. The TEM analysis led us to hypothesize that VLVs are abnormal primary virions mislocalized into cytoplasmic membranes. This hypothesis predicts that pUL34, which is a structural component of the primary but not the mature virion (14, 27, 31, 42, 45), should also be redistributed from the nuclear rim to the cytoplasm in PC6-3 cells overexpressing TAwt but not TAmut. Furthermore, pUL34 mislocalization should be dependent on capsid formation, and there should be, to some extent, association between capsids and cytoplasmic pUL34. To test these predictions, PC6-3TAwt or PC6-3TAmut cells were mock or DOX induced for 14 h and then infected with 5 PFU/cell of HSV-1(F) or VP5-null virus. Sixteen hours after infection, cells were fixed in paraformaldehyde and permeabilized, and localization of pUL34 was determined by indirect immunofluorescence (IF) (Fig. 3A and B). In uninduced PC6-3 cells infected with HSV-1 or VP5-null virus, pUL34 was localized to the nuclear rim. Additional fine reticular cytoplasmic pUL34 localization was observed in about half of the cells (Fig. 3Aa and c and Ba). In contrast, in cells in which TAwt expression was induced, pUL34 mislocalized to cytoplasmic puncta in about 40% of cells (Fig. 3Ad). pUL34 puncta were not observed in TAmut-overexpressing cells (Fig. 3Af), suggesting that the formation of pUL34 cytoplasmic puncta is specifically associated with functional torsinA overexpression. Redistribution of pUL34 was not due to global NE disruption because localization of another INM marker, lamin-associated protein 2 (LAP2), was unchanged in infected cells that had been induced to express TAwt (Fig. 3A, compare b and e). In addition, cytoplasmic pUL34 puncta were rarely observed in VP5-null virus-infected cells (Fig. 4Bb), indicating their dependence on capsid formation.

To test the prediction that mislocalized pUL34 puncta are associated with capsids, we took advantage of a recombinant HSV-1 BAC in which a monomeric RFP is fused to a small outer capsid protein (VP26). To determine if pUL34 puncta and cytoplasmic VP26 colocalize, uninduced or DOX-induced PC6-3TAwt cells were infected with rHSVBAC35R at an MOI of 5 for 16 h and then immunofluorescently stained to detect pUL34 (Fig. 3C). Capsids visualized as RFP puncta (11) were easily detectable throughout both uninduced and DOX-induced rat cells (Fig. 3Cb and d). Under both experimental

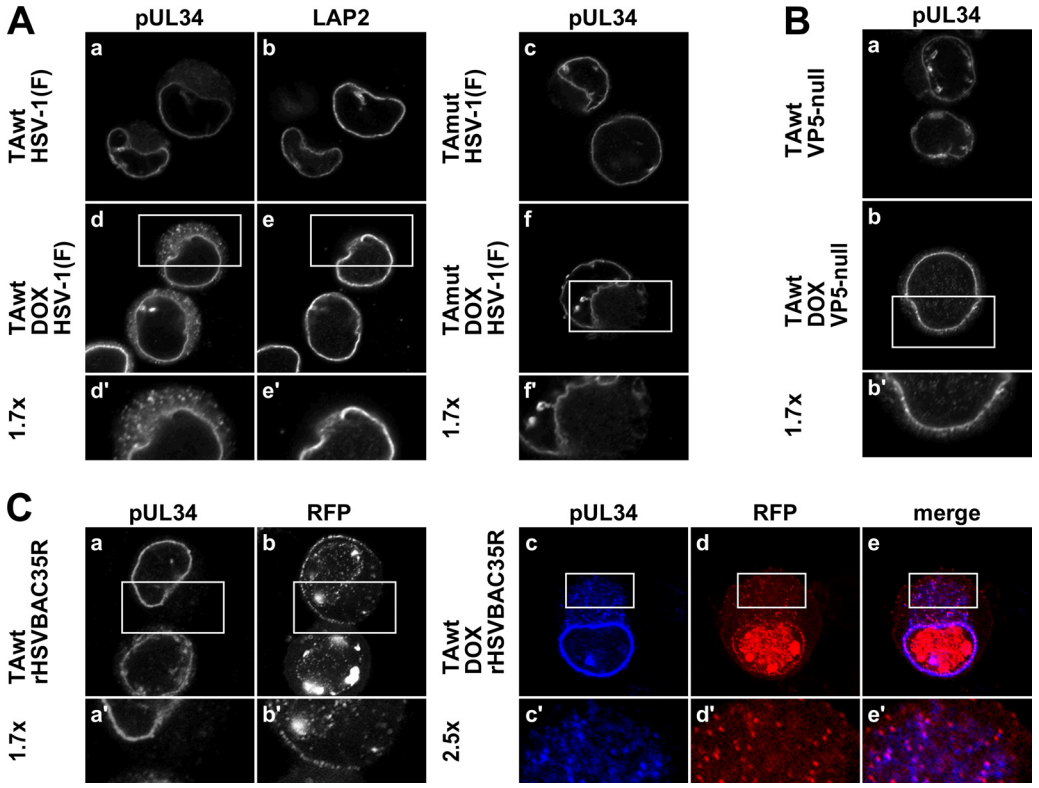

FIG. 3. Overexpression of TAwt leads to formation of pUL34 puncta in the cytoplasm. Representative confocal immunofluorescence images are shown. (A) Formation of cytoplasmic pUL34 puncta in TAwt- but not TAmut-overexpressing cells. PC6-3-TAwt (a, b, d, and e) and PC6-3-TAmut (c and f) cells were mock (a to c) or DOX treated (d to f) for 14 h and then infected with HSV-1(F) at an MOI of 5 for 16 h. The visualized protein is indicated on the top of the image. (B) Formation of pUL34 puncta depends on capsid formation. Uninduced (a) or DOX-treated (b) PC6-3-TAwt cells were infected with VP5-null virus and stained for pUL34. (C) pUL34 puncta colocalize with a capsid protein. Mock-treated (a and b) or DOX-treated (c to e) PC6-3-TAwt cells were infected with rHSVBAC35R and stained for pUL34 (a and c). RFP-VP26 was detected by RFP fluorescence (b and d). Boxed areas are shown at magnifications of ×1.7 and ×2.5, as indicated.

conditions there was considerable cell-to-cell variation in the number and distribution of capsids. Staining patterns for pUL34 expressed from rHSVBAC35R or HSV-1(F) were very similar (compare Fig. 3Aa and d and Ca and c). The majority of cytoplasmic pUL34 puncta that form in DOX-induced cells colocalized with RFP puncta (Fig. 3Cc to e). Furthermore, pUL34 puncta did not colocalize at the cell periphery with RFP puncta, which most likely represent mature virions at the cell surface (Fig. 3Cc to e). These data strongly suggested that structures detected as pUL34 puncta represent primary virions that abnormally accumulate in the cytoplasm. To estimate fractions of colocalizing pUL34 and RFP puncta, respectively, pUL34 and RFP puncta were counted in 14 DOX-induced cells that displayed pUL34 mislocalization (Table 2). The great majority (90%) of cytoplasmic pUL34 puncta colocalize with RFP puncta, indicating that a much higher percentage of VLVs contain capsid proteins than anticipated from the TEM analysis. Quantification also showed that, on average, one-third of RFP puncta outside the nucleus did not colocalize with pUL34 puncta, indicating that the normal process of capsid de-envelopment at the NE still occurs to some extent in these cells (Table 2).

pUL34 immunogold labeling of virion-like structures in the cytoplasm of torsinA wild-type-overexpressing cells. Ultrastructural and immunofluorescence data cumulatively suggested that primary virions that contain pUL34 accumulate in the cytoplasm when TAwt is overexpressed. To further support this hypothesis, pUL34 immunogold labeling was performed on cryosections prepared from mock- or DOX-induced PC6-3TAwt cells that were infected with HSV-1(F) for 20 h (Fig. 4). Cell preservation and pUL34 immunogold labeling of the nuclear rim are shown in Fig. 4A and B, respectively. Virions, with distinct darker cores, clearly defined membranous outer layers, and diameters of between 0.16 and 0.22 μm, were rarely seen in the cytoplasm (Fig. 4Ca) but often on the cell surface (Fig. 4Cb) of uninduced cells. Furthermore, no immunogold labeling of virions for pUL34 was observed in these cells. In TAwt-overexpressing cells, gold beads were observed near or inside cytoplasmic structures that resemble virions in size and in the appearance of the capsid and core (Fig. 4Da). Surface virions that were occasionally detected in DOX-induced cells did not stain for pUL34 (Fig. 4Db). This experiment thus verified the presence of pUL34-positive virion-like structures in the cytoplasm.

HSV-1 infection redistributes torsinA wild type into puncta that colocalize with pUL34 and a capsid protein. The apparent change in the fate of primary virions in TAwt-expressing cells could be due to an indirect effect of TAwt-mediated changes in NE or ER function or to a specific functional interaction with the primary virion. To determine if HSV-1 infection changes

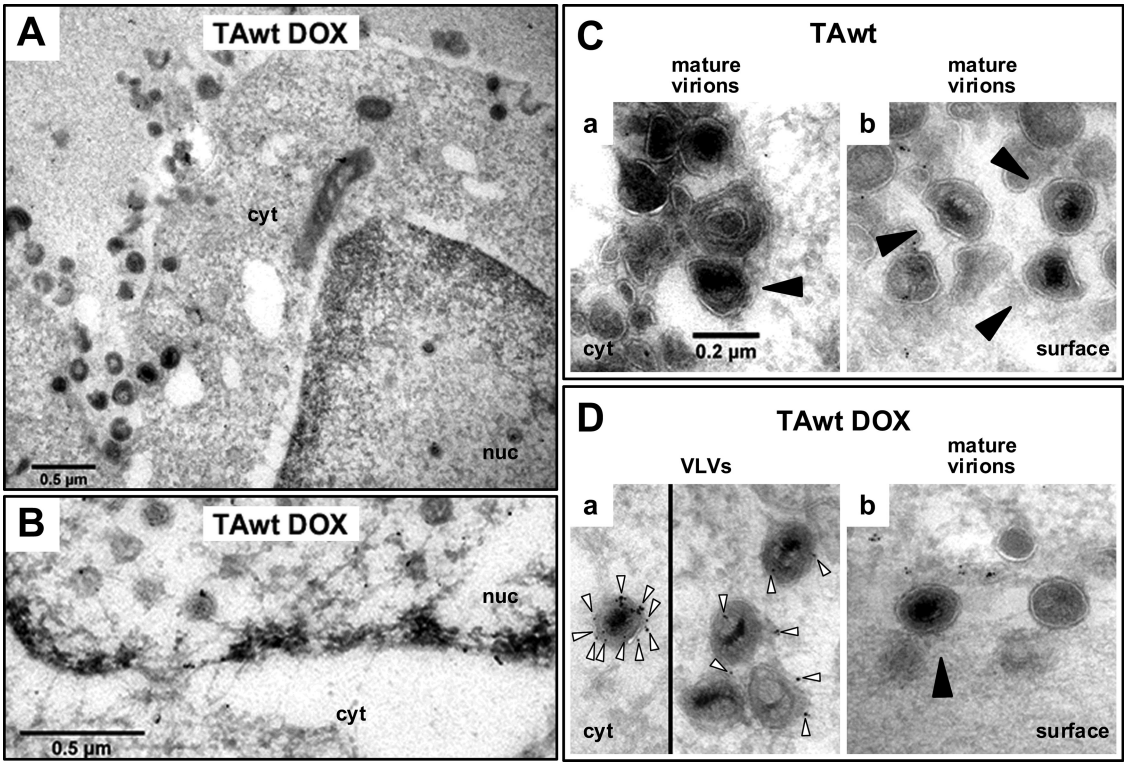

FIG. 4. Electron micrographs of pUL34 immunogold-labeled cryosections of PC6-3-TAwt cells. Ultrathin cryosections prepared from HSV-1(F)-infected mock-treated (C) or DOX-treated (A, B, and D) PC6-3TAwt cells were immunogold labeled for pUL34 and viewed by TEM as described in Material and Methods. (A) General cell morphology. (B) Immunogold detection of pUL34 at the nuclear envelope. (C) In uninduced cells, virions (black arrowhead) in the cytoplasm (a) or at the cell surface (b) did not stain for pUL34. (D) In TAwt-overexpressing cells, gold grains (white arrows) were observed in proximity or inside virion-like structures in the cytoplasm (a) but not at the site of surface virions (black arrowhead) (b). All images in panels C and D are shown at the same magnification.

TA localization, uninduced or DOX-induced PC6-3TAwt or PC6-3TAmut cells were infected for 16 h with HSV-1(F), and then localization of TA was determined by IF (Fig. 5A). In uninfected cells TAwt was distributed in a fine reticular pattern in the cytoplasm (Fig. 5Aa). Infection with HSV-1 caused TA to adopt a more punctate appearance in the cytoplasm or show a greater concentration at the nuclear rim in most cells (≈90%) (Fig. 5Ac).

TAmut localization differed from that of TAwt in uninfected cells in that TAmut concentrated near the nuclear rim, and in cells that expressed exceptionally high levels, additional TAmut inclusions were observed in the cytoplasm (Fig. 5Ab), as previously reported in these cells (17). Infection with HSV-1 did not change TAmut localization (Fig. 5A, compare b and d).

TABLE 2. Number and percentages of colocalizing puncta in HSV-1(F)-infected DOX-induced PC6-3TAwt cells[a]

Protein	Avg no. of puncta per cell	Colocalization of puncta with pUL34 (%)	Colocalization of puncta with RFP (%)	Colocalization of puncta with TAwt (%)
pUL34	39.7		90.3	85.1
RFP-VP26	55.2	66.2		67.7
TAwt	41.5	86.2	83.6	

[a] Confocal images of 14 cells that showed cytoplasmic pUL34 puncta were selected and counted for the number of colocalizing puncta and puncta that did not colocalize.

Formation of cytoplasmic TA puncta was dependent on pUL34 and VP5 expression since the TAwt puncta were not observed in cells infected with UL34-null or VP5-null virus (Fig. 5B). This indicates that capsid primary envelopment is required for the formation of TAwt puncta in the cytoplasm. Infection with the deletion viruses did not, however, restore TAwt distribution to that of the uninfected cells because cells with an accumulation of TAwt close to the nuclear rim were still commonly observed (Fig. 5Ba and b).

Merging images from DOX-induced PC6-3TAwt cells that were infected with rHSVBAC35R and immunofluorescently stained to detect TAwt and pUL34 (as shown in Fig. 3C) showed that more than 80% of TAwt puncta visibly overlapped with pUL34 and/or RFP puncta (Fig. 5C and Table 2). The extensive colocalization of TAwt with primary virions in the cytoplasm raised the possibility TAwt is associated with the primary virion and has a functional role in virion nuclear egress.

To ask if HSV-1 infection alters the accumulation and post-translational modification of TA, uninduced or DOX-induced PC6-3TAwt cells were mock or HSV-1(F) infected for 12 h, and whole-cell lysate was immunoblotted for human TA. As seen in Fig. 5D, infection did not change the intensity or migration patterns of overexpressed human TA, indicating that infection does not affect TA protein levels or posttranslational modifications.

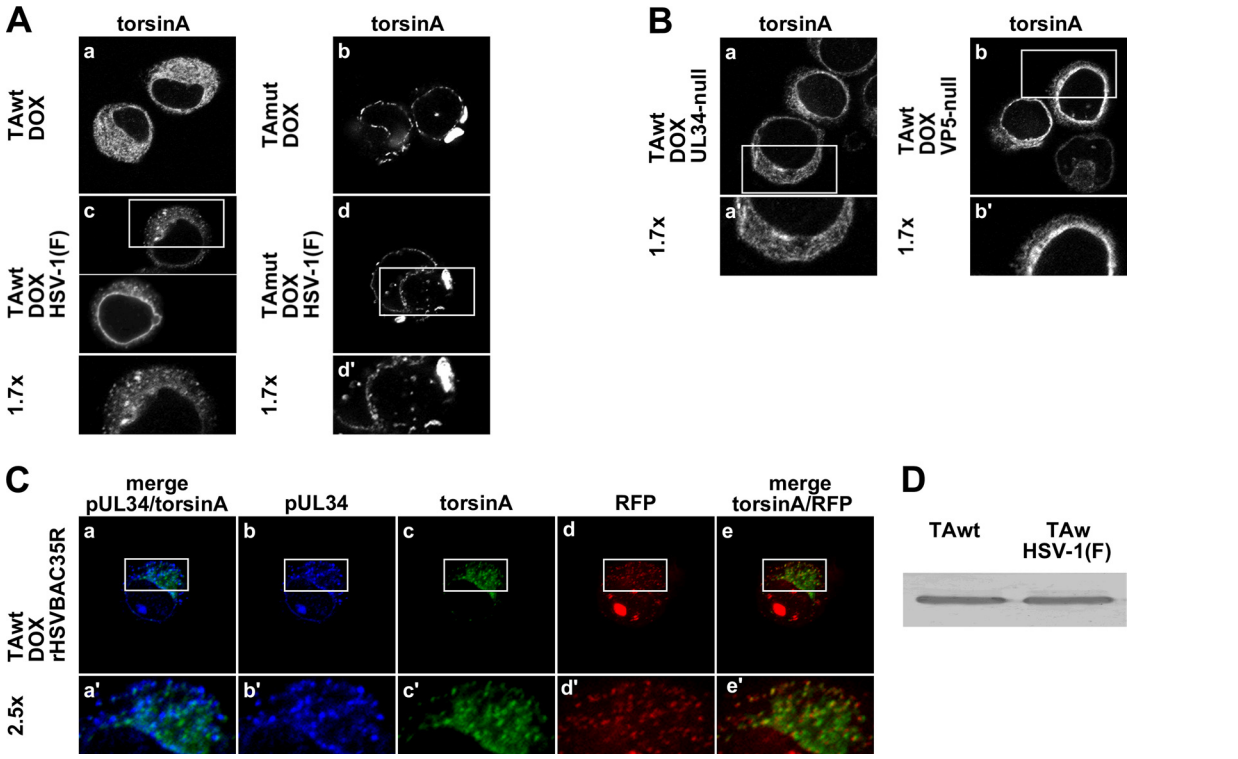

FIG. 5. Consequence of HSV infection on TA. (A) HSV-1 infection redistributes TAwt but not TAmut. Shown are confocal images of DOX-induced PC6-3TAwt (a and c) or PC6-3TAmut (b and d) cells that were infected with mock virus (a and b) or HSV-1(F) (c and d) and immunofluorescently stained for human TA. (B) Formation of cytoplasmic TAwt puncta depends on capsid formation and primary envelopment. PC6-3TAwt cells induced to express TAwt were infected with UL34-null (a) or VP5-null (b) virus and stained for human TA (a and b) and a virus protein to verify infection (data not shown). (C) TAwt puncta colocalization with pUL34 puncta and a capsid protein. DOX-treated PC6-3TAwt cells were infected with rHSVBAC35R and visualized for TAwt (c), pUL34 (b), and RFP (d). Boxed areas are shown at magnifications of ×1.7 and ×2.5, as indicated. (D) Western blot for overexpressed human TA. PC6-3-TAwt cells were DOX treated for 14 h and then infected with mock virus (left lane) or HSV-1(F) (right lane) at 5 PFU/cell for 12 h.

TorsinA and torsinB overexpression interferes with the HSV-1 life cycle in 293T and Vero cells. To test if the HSV-1 growth defect in a rat neuronal cell line overexpressing TAwt was cell type specific, we measured virus production in 293T cells that were transfected to express GFP-tagged torsinA. Additionally, we also asked if overexpression of torsinB, whose function overlaps with TA function at the NE, has the same inhibitory effect on virus production as TAwt. The GFP-tagged versions of TA and TB have been shown to be functional and to localize properly (18, 25, 39). For this experiment, 293T cells were transfected with GFP, GFP-TAwt, or GFP-TB and 24 h later infected with HSV-1(F) at an MOI of 5. Virus production was measured at 16 h after infection (Fig. 6A). Overexpression of GFP-TAwt and GFP-TB significantly decreased virus production ($P < 0.0001$) compared to control levels, suggesting that the growth defect caused by TAwt overexpression is not restricted to rat neuronal cells and also that TB overexpression has a similar inhibitory effect on HSV-1 production.

To determine the fate of pUL34 in nonrat cells that overexpressed torsin, Vero cells were transfected with GFP, GFP-TAwt, or GFP-TB and infected 24 h later with mock virus or HSV-1(F). Cells were assayed at 16 h for localization of GFP, GFP fusions, and pUL34 by IF (Fig. 6B). As expected, HSV-1 infection did not significantly change GFP localization, except for the occasional appearance of GFP puncta in the nucleus (Fig. 6B, compare a and d), and GFP expression did not alter the typical nuclear rim localization of pUL34 (Fig. 7Be).

In uninfected Vero cells, GFP-TAwt was found at the nuclear rim and in a smooth reticular and punctate distribution in the cytoplasm (Fig. 6Bg). In about 90% of transfected cells, GFP-TAwt was redistributed upon infection such that it was either found closer to the NE or it became more punctate in the cytoplasm (Fig. 6B, compare g and j). As seen in PC6-3 cells, pUL34 formed cytoplasmic puncta in about 40% of the cells that expressed the TAwt construct. In addition, uneven pUL34 staining on the nuclear rim was commonly observed (Fig. 6, compare e and k). Also similar to what was seen in PC6-3 cells, most pUL34 puncta also contained TAwt puncta (Fig. 6Bl′). Furthermore, when capsids were visualized by using the rHSVBAC35R virus, extensive colocalization between pUL34, RFP-VP26, and GFP-TAwt was observed (data not shown). These data imply that interference of TA normal function by overexpression leads to nuclear egress defects in multiple cells lines.

Distribution of GFP-TB is distinct from that of GFP-TA in Vero cells as GFP-TB is primarily found at the nuclear rim. At higher expression levels, additional aggregates are observed in the cytoplasm (Fig. 6Bm). In infected cells redistribution of pUL34 due to GFP-TB expression is indistinguishable from that caused by GFP-TAwt expression (Fig. 6q). Infection also

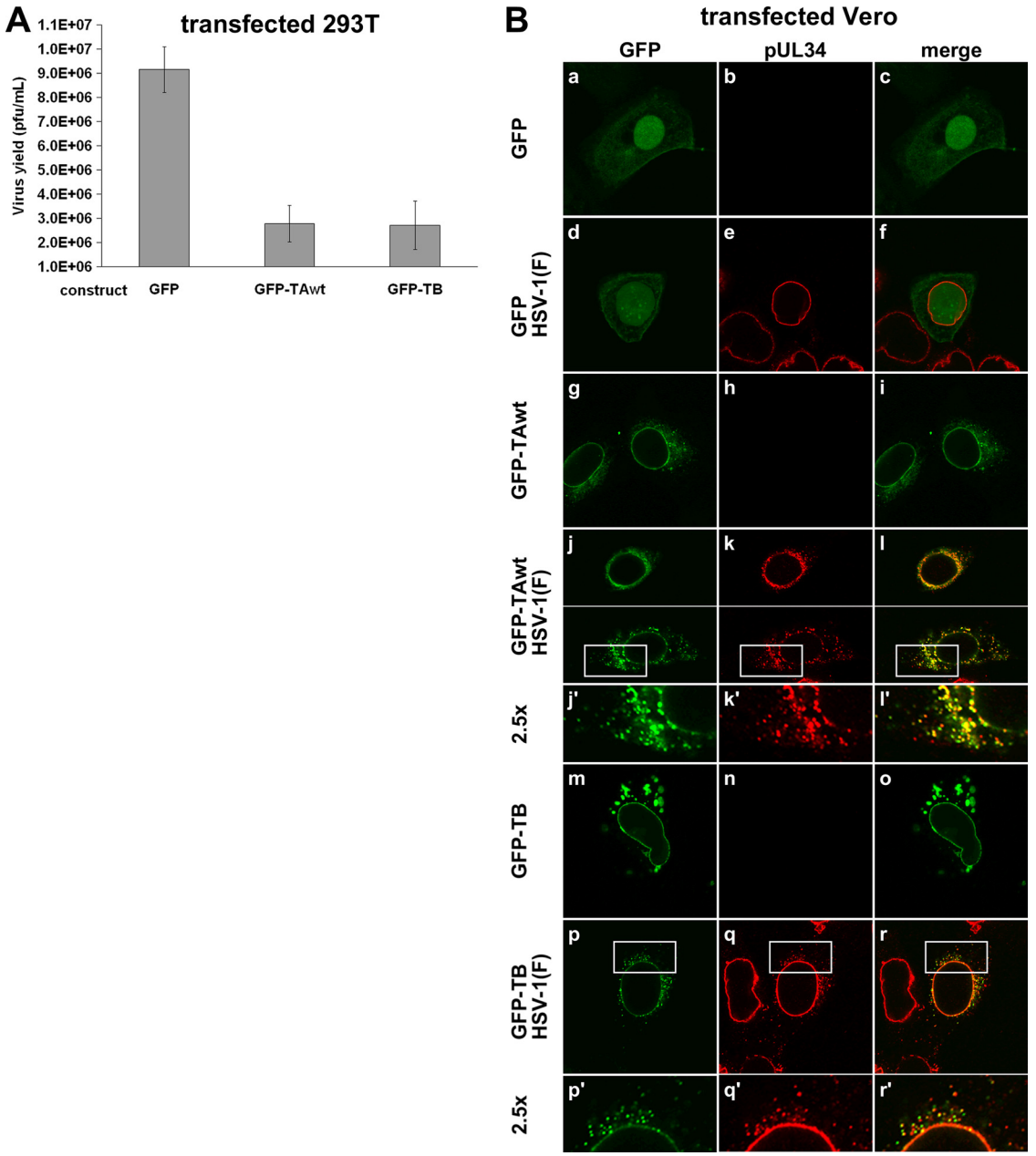

FIG. 6. Overexpression of TAwt and TB interferes with the HSV-1 life cycle in 293T and Vero cells. (A) Impairment of HSV-1 replication in 293T cells overexpressing TAwt and TB. 293T cells were transfected with the indicated GFP constructs and 24 h later infected with HSV-1(F) at an MOI of 5. Virus titers were determined on Vero cells at 16 hpi. Each histogram represents the mean value of four experiments. Error bars indicate the sample standard deviations. (B) Formation of cytoplasmic pUL34 in Vero cells that overexpressed TAwt or TB. Shown are confocal images of Vero cells that were transfected with the indicated GFP constructs (at left), incubated for 24 h, and then infected with HSV-1(F) at an MOI of 5. At 16 hpi cells were visualized for pUL34 and GFP expression. Boxed areas are shown at a magnification of ×2.5.

changed the appearance of GFP-TB, which appeared punctate in the cytoplasm (Fig. 6Bp). As seen in Fig. 6r′, pUL34 and GFP-TB puncta partially colocalize, thus further supporting the idea that overexpression of these two torsin homologs has the same consequences for the HSV-1 life cycle.

pUL34 puncta colocalize with an ER marker. Primary virions that form in the perinuclear space do not normally enter the ER lumen, despite the continuity of these two compartments. TA is a fully translocated ER protein with biochemical properties of a peripheral protein that shows extensive colocalization with common ER markers (5, 15, 25). Colocalization of TAwt with pUL34 led us to hypothesize that primary virions are found in the ER when TAwt is overexpressed or, alternatively, that HSV infection might change the normal TAwt distribution. To distinguish between these two possibilities, Vero cells, chosen because of their large cytoplasms, were transfected with GFP-TAwt and RFP-KDEL (RFP fused to a classical ER retention signal) and mock infected or infected

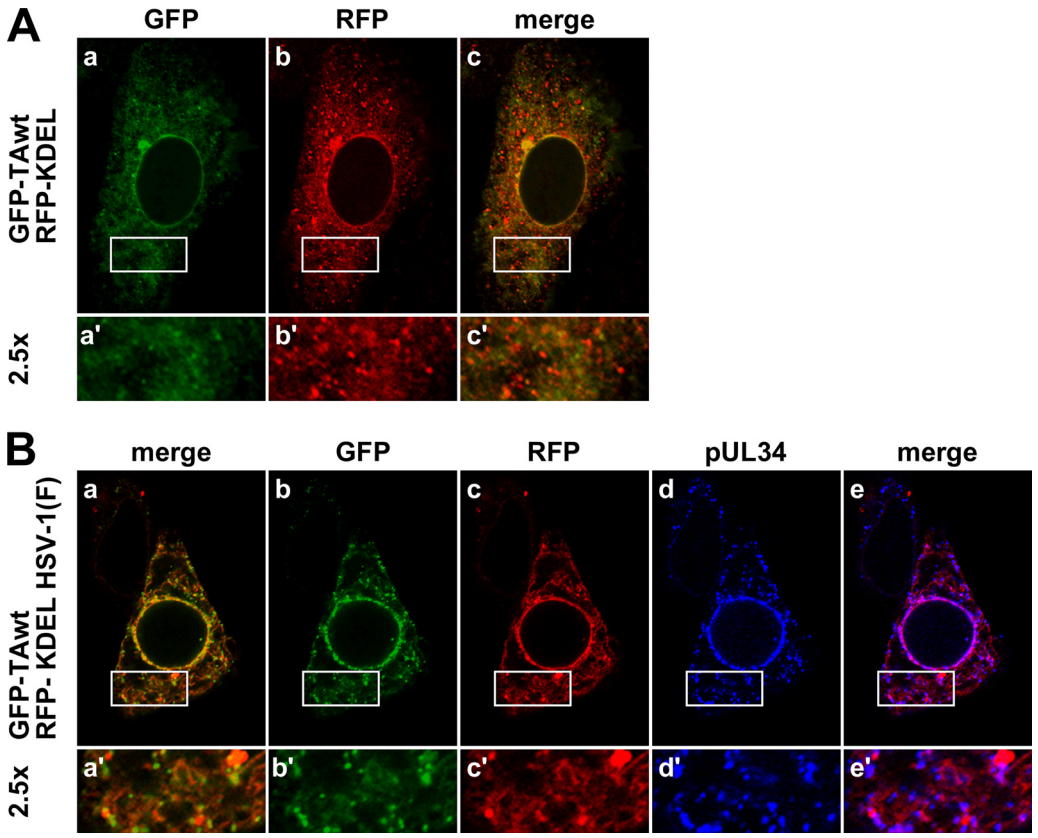

FIG. 7. pUL34 puncta are associated with the ER. Vero cells were transfected with GFP-TAwt and RFP-KDEL and 35 h later infected with mock virus (A) or HSV-(1F) at an MOI of 5 (B). Infection was left to proceed for 16 h before the cells were immunofluorescently stained for pUL34. Boxed areas are shown at a magnification of ×2.5.

with HSV-1(F) 35 h later. At 16 hpi localization of GFP, RFP, and pUL34 was determined (Fig. 7). In uninfected Vero cells, the ER compartment revealed smooth to punctate localization of GFP-TAwt and RFP-KDEL, as shown in Fig. 7Aa and b, respectively. While both proteins follow very similar patterns of distribution, local areas of concentration of each protein only occasionally coincide (Fig. 7Ac), indicating that these two proteins preferentially accumulate in different parts of the ER. This remains true in HSV-1-infected cells, where TAwt and RFP-KDEL still show very similar distribution patterns (Fig. 7Ba to c) but where local areas of concentration still do not coincide (note numerous individual red and green puncta in the merged image in Fig. 7Ba′). The same localization pattern is observed for pUL34 (Fig. 7Bc to e), whose cytoplasmic distribution extensively overlaps that of RFP-KDEL (note magenta indicating colocalization in Fig. 7Be), but local concentrations (puncta) of RFP-KDEL and pUL34 generally do not colocalize. This is unsurprising since no specific association is expected between primary virions and RFP-KDEL. These data suggest that pUL34 puncta reside within the ER compartment.

DISCUSSION

The effect of TA overexpression on TA function. Overexpression of a wild-type protein can perturb its function by either increasing or inhibiting its normal function. Functional enhancement has been observed with some enzymes, transcription factors, and chaperones. Examples of proteins whose function is inhibited by overexpression include Rab11-Fip2, TSG101, and Rip11 (10, 16, 57, 61), and while the mechanisms are not always known, one could imagine a scenario in which overexpressed wild-type protein may disrupt its own function by sequestering and/or relocalizing its binding partner(s). TA is a multifunctional protein for which different activities are affected differently by overexpression. For example, overexpression of TAwt was found to inhibit formation of protein aggregates, to reduce an induced ER stress response, and to enhance protein processing through the secretory pathway—effects suggesting enhancement of TA chaperone function (3, 6, 8, 20, 23, 29, 33, 51, 58). On the other hand, at least one of TA functions is disrupted by its overexpression. Blebs at the NE observed in neurons when TAwt was overexpressed or when TA was absent appeared very similar, suggesting that overexpression negates a TA function important for maintaining normal nuclear architecture (19, 26).

We cannot say whether the inhibition of de-envelopment and mislocalization of primary virions observed here are due to enhancement or inhibition of TAwt function. We observed blebbing of the nuclear envelope (Fig. 2A) similar to that seen in neurons that cannot express TA. This suggests that at least one TAwt function is inhibited, and our phenotypes might be explained by TAwt sequestering cellular or virus components essential for primary virion de-envelopment. However, the vi-

ral replication, de-envelopment, and virion mislocalization phenotypes we observed were induced by expression of wild-type but mot mutant TA. This suggests that these phenotypes depend upon TA activity and might result from enhancement of a novel TA function that negatively regulates fusion of the perinuclear virion envelope with the ONM.

Origin and location of VLVs. Three considerations suggest that the VLVs observed by TEM are the same structures as the cytoplasmic UL34 puncta observed by immunofluorescence: (i) structures appear in TAwt, but not TAmut overexpressing PC6-3, (ii) both structures show the same dependence on capsid protein expression, and (iii) UL34-containing virion-like structures are found in the cytoplasm in immunogold labeling with TEM. That VLVs are virions is suggested by their size and the presence of morphologically discernible capsids or VP26 puncta in TEM or immunofluorescence assays, respectively. Despite their clear dependence on capsid protein expression, capsids were indistinct or not visible in more than half of the VLVs observed in TEM (Table 1). The association of the vast majority (90%) of pUL34 puncta with a capsid protein (RFP-VP26) (Table 2) suggests, however, that more VLVs contain capsids than anticipated by the TEM analysis. The difficulty in visualizing capsids in VLVs might be due to the internal environment of VLVs, which may differ from that of normal primary virions in a way that either masks or destabilizes the organization of capsids. Whether the remainder of pUL34 puncta (about 10%) that do not obviously associate with RFP-VP26 actually do not contain a capsid or for some reason do not associate with the RFP-tagged capsids protein is unclear and difficult to address.

Ordinarily, the only enveloped virion structures in the cytoplasm are mature virions that have undergone secondary envelopment and are in envelopment or transport compartments. VLVs, however, are clearly distinct from mature virions and have characteristics typical of primary virions derived from envelopment at the INM. First, the envelope of mature virions has a characteristic fuzzy appearance in TEM due to the presence of virion envelope proteins projecting from the exterior of the membrane, whereas primary virions have a sharp, electron-dense membrane. The VLV membrane is typical of primary rather than mature virions (Fig. 2D, compare panels g and h with b or c and i). Most important, primary virions are distinguished biochemically by the presence of the viral pUL31 and pUL34 proteins, which are absent from mature virions and from most cytoplasmic membranes (14, 27, 31, 42, 42, 45). The concentration of pUL34 in VLVs strongly suggests that these structures are primary virions that are localized in cytoplasmic membranes.

The number of VLVs greatly exceeds the number of primary perinuclear virions seen in cells that do not overexpress TAwt (Table 1). Accumulation of VLVs thus suggests that de-envelopment of these particles is inhibited and that normal TA function may be required for efficient de-envelopment fusion. Inhibition of de-envelopment has also been observed in cells infected with viruses that fail to express either pUS3 or both gB and gH (13, 28, 45). In these cases, however, the accumulated primary virions are found in an expanded perinuclear space (for gB/gH deletion) or in a space created by invagination of the INM (for US3 deletion). Neither in wild-type infection nor in either of these deletions are structures resembling primary virions found in cytoplasmic structures like VLVs.

In electron micrographs, cytoplasmic VLVs were surrounded by an additional membrane (Fig. 2Dg and h). The origin of the outer membrane is unclear, but the following observations lead us to hypothesize that the membrane might derive from the ER: (i) the outer membrane of VLVs has an irregular, sometimes tubular shape (Fig. 2Dh), (ii) perinuclear VLVs were observed between perinuclear space and what appears to be an ER tubule (data not shown), (iii) in the cytoplasm pUL34/RFP-VP26 puncta colocalize with TAwt puncta (Fig. 5C), which is an ER luminal protein, and it appears to remain in the ER after HSV-1 infection (Fig. 7), and (iv) UL34/TAwt puncta show the same distributions as ER membranes in infected cells (Fig. 7B). Normally, primary virions do not enter the ER lumen despite the continuity of the perinuclear space and the ER lumen. The reasons for this are not clear, but it appears that the ER luminal compartment is somehow closed to primary virions. This apparently remains true when de-envelopment fusion is inhibited by deletion of pUS3 or gB and gH. The presence of VLVs in the ER lumen when normal TA function is disrupted by overexpression raises the possibility that normal TA function is required for exclusion of perinuclear virions from the ER lumen.

The extensive colocalization of TA with pUL34 and a capsid protein in cytoplasmic puncta in cells that overexpress TAwt and the dependence of TA/pUL34 colocalization on capsid envelopment raise the possibility that TAwt is physically associated in these cells with the inner membrane of VLVs (i.e., the membrane equivalent to the perinuclear virion envelope). This association is unlikely to result from direct interaction with pUL34 since the ER luminal extension of pUL34 consists of only a few amino acids (52). More likely, TAwt associates with the extracellular/luminal domain of viral or cellular proteins inserted into the primary virion envelope. For the virus, these proteins include at least gD, gM (1, 55), and possibly gB (59). The presence of gH in the perinuclear virion has not been demonstrated biochemically but is likely, given its role in de-envelopment fusion in HSV. Since our results suggest that normal TA function is required for de-envelopment fusion, it is tempting to speculate that TA association with proteins of the viral fusion apparatus might be important for this function.

Collectively, our studies suggest the model depicted in Fig. 8. Normally during HSV-1 infection, capsids become enveloped at the INM, forming short-lived primary virions in the perinuclear space. Overexpression of TAwt impairs the de-envelopment of primary virions, possibly by inhibiting their fusion with the ONM and opening the ER lumen to these particles, where they become trapped in ER tubules and are unable to mature and egress from the cell. It is also possible that primary envelopment proceeds normally, and capsids form VLVs by enveloping into a TAwt/pUL34-modified cytoplasmic membrane. This model could explain cytoplasmic VLVs but not the presence of perinuclear VLVs.

TA is thought to participate in organization of the NE through at least two pathways. In one pathway, TA interacts with the INM transmembrane lamin-associated protein 1 (LAP1), and disruption of the TA-LAP1 pathway leads to abnormal invaginations of the INM into perinuclear space (19, 26). Interestingly, in a second pathway, TA was shown to bind

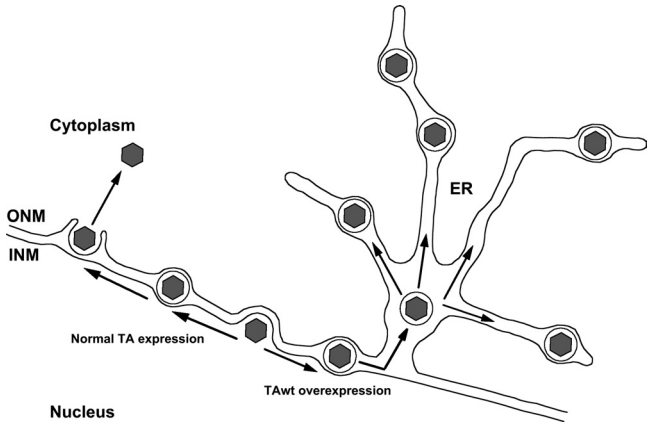

FIG. 8. Model of HSV-1 nuclear egress in TAwt-overexpressing cells. During the course of HSV-1 infection, capsids exit the nucleus by budding at the INM. This process leads to formation of enveloped primary virions in the perinuclear space which then de-envelope by fusing with the ONM. TAwt overexpression impairs the de-envelopment process of primary virions and promotes their entry into the ER lumen.

nesprin-3α and as such may regulate Sun-nesprin interactions, which are thought to contribute to uniform perinuclear spacing (9, 40, 60). One possible interpretation of our results is that perinuclear virions produced in a normal infection are unable to enter the ER lumen because their movement in the perinuclear space is sterically restricted by interactions between Sun and nesprin proteins. Interference with torsin function may disrupt these interactions, thereby liberating the perinuclear virions for movement through the perinuclear space to the ER. Our results, then, suggest two novel functions of torsin family members at the NE: regulation of membrane fusion and regulation of the transition from perinuclear space to ER lumen. Our study also shows that HSV infection provides a uniquely useful window into functions for torsin family members.

ACKNOWLEDGMENTS

We thank Jean Ross from the Central Microscopy Research Facilities of the University of Iowa for expert technical assistance with TEM. We are also grateful to Wendy Maury (University of Iowa) for critically reading the manuscript.

These studies were supported by Public Health Service grants AI41478 and K02NS058450 awarded to R.J.R and P.G.-A., respectively.

REFERENCES

1. **Baines, J. D., E. Wills, R. J. Jacob, J. Pennington, and B. Roizman.** 2007. Glycoprotein M of herpes simplex virus 1 is incorporated into virions during budding at the inner nuclear membrane. J. Virol. **81:**800–812.
2. **Bjerke, S. L., and R. J. Roller.** 2006. Roles for herpes simplex virus type 1 UL34 and US3 proteins in disrupting the nuclear lamina during herpes simplex virus type 1 egress. Virology **347:**261–276.
3. **Burdette, A. J., P. F. Churchill, G. A. Caldwell, and K. A. Caldwell.** 2010. The early-onset torsion dystonia-associated protein, TorsinA, displays molecular chaperone activity in vitro. Cell Stress Chaperones **15:**605–617.
4. **Caldwell, G. A., et al.** 2003. Suppression of polyglutamine-induced protein aggregation in *Caenorhabditis elegans* by torsin proteins. Hum. Mol. Genet. **12:**307–319.
5. **Callan, A. C., S. Bunning, O. T. Jones, S. High, and E. Swanton.** 2007. Biosynthesis of the dystonia-associated AAA^+ ATPase TorsinA at the endoplasmic reticulum. Biochem. J. **401:**607–612.
6. **Cao, S., C. C. Gelwix, K. A. Caldwell, and G. A. Caldwell.** 2005. Torsin-mediated protection from cellular stress in the dopaminergic neurons of *Caenorhabditis elegans*. J. Neurosci. **25:**3801–3812.
7. **Chang, Y. E., C. Van Sant, P. W. Krug, A. E. Sears, and B. Roizman.** 1997. The null mutant of the U_L31 gene of herpes simplex virus 1: construction and phenotype in infected cells. J. Virol. **71:**8307–8315.
8. **Chen, P., et al.** 2010. The early-onset torsion dystonia-associated protein, TorsinA, is a homeostatic regulator of endoplasmic reticulum stress response. Hum. Mol. Genet. **19:**3502–3515.
9. **Crisp, M., et al.** 2006. Coupling of the nucleus and cytoplasm: role of the LINC complex. J. Cell Biol. **172:**41–53.
10. **Cullis, D. N., B. Philip, J. D. Baleja, and L. A. Feig.** 2002. Rab11-FIP2, an adaptor protein connecting cellular components involved in internalization and recycling of epidermal growth factor receptors. J. Biol. Chem. **277:**49158–49166.
11. **de Oliveira, A. P., et al.** 2008. Live visualization of herpes simplex virus type 1 compartment dynamics. J. Virol. **82:**4974–4990.
12. **Desai, P., N. A. DeLuca, J. C. Glorioso, and S. Person.** 1993. Mutations in herpes simplex virus type 1 genes encoding VP5 and VP23 abrogate capsid formation and cleavage of replicated DNA. J. Virol. **67:**1357–1364.
13. **Farnsworth, A., et al.** 2007. Herpes simplex virus glycoproteins gB and gH function in fusion between the virion envelope and the outer nuclear membrane. Proc. Natl. Acad. Sci. U. S. A. **104:**10187–10192.
14. **Fuchs, W., B. G. Klupp, H. Granzow, N. Osterrieder, and T. C. Mettenleiter.** 2002. The interacting UL31 and UL34 gene products of pseudorabies virus are involved in egress from the host-cell nucleus and represent components of primary enveloped but not mature virions. J. Virol. **76:**364–378.
15. **Giles, L. M., J. Chen, L. Li, and L. S. Chin.** 2008. Dystonia-associated mutations cause premature degradation of torsinA protein and cell-type-specific mislocalization to the nuclear envelope. Hum. Mol. Genet. **17:**2712–2722.
16. **Goila-Gaur, R., D. G. Demirov, J. M. Orenstein, A. Ono, and E. O. Freed.** 2003. Defects in human immunodeficiency virus budding and endosomal sorting induced by TSG101 overexpression. J. Virol. **77:**6507–6519.
17. **Gonzalez-Alegre, P., and H. L. Paulson.** 2004. Aberrant cellular behavior of mutant TorsinA implicates nuclear envelope dysfunction in DYT1 dystonia. J. Neurosci. **24:**2593–2601.
18. **Goodchild, R. E., and W. T. Dauer.** 2004. Mislocalization to the nuclear envelope: an effect of the dystonia-causing torsinA mutation. Proc. Natl. Acad. Sci. U. S. A. **101:**847–852.
19. **Goodchild, R. E., C. E. Kim, and W. T. Dauer.** 2005. Loss of the dystonia-associated protein torsinA selectively disrupts the neuronal nuclear envelope. Neuron **48:**923–932.
20. **Gordon, K. L., K. A. Glenn, and P. Gonzalez-Alegre.** 2011. Exploring the influence of torsinA expression on protein quality control. Neurochem. Res. **36:**452–459.
21. **Granata, A., G. Schiavo, and T. T. Warner.** 2009. TorsinA and dystonia: from nuclear envelope to synapse. J. Neurochem. **109:**1596–1609.
22. **Grundmann, K., et al.** 2007. Overexpression of human wild-type torsinA and human ΔGAG torsinA in a transgenic mouse model causes phenotypic abnormalities. Neurobiol. Dis. **27:**190–206.
23. **Hewett, J. W., et al.** 2008. siRNA knock-down of mutant torsinA restores processing through secretory pathway in DYT1 dystonia cells. Hum. Mol. Genet. **17:**1436–1445.
24. **Hewett, J. W., et al.** 2007. Mutant torsinA interferes with protein processing through the secretory pathway in DYT1 dystonia cells. Proc. Natl. Acad. Sci. U. S. A. **104:**7271–7276.
25. **Jungwirth, M., M. L. Dear, P. Brown, K. Holbrook, and R. Goodchild.** 2010. Relative tissue expression of homologous torsinB correlates with the neuronal specific importance of DYT1 dystonia-associated torsinA. Hum. Mol. Genet. **19:**888–900.
26. **Kim, C. E., A. Perez, G. Perkins, M. H. Ellisman, and W. T. Dauer.** 2010. A molecular mechanism underlying the neural-specific defect in torsinA mutant mice. Proc. Natl. Acad. Sci. U. S. A. **107:**9861–9866.
27. **Klupp, B. G., H. Granzow, and T. C. Mettenleiter.** 2000. Primary envelopment of pseudorabies virus at the nuclear membrane requires the UL34 gene product. J. Virol. **74:**10063–10073.
28. **Klupp, B. G., H. Granzow, and T. C. Mettenleiter.** 2001. Effect of the pseudorabies virus US3 protein on nuclear membrane localization of the UL34 protein and virus egress from the nucleus. J. Gen. Virol. **82:**2363–2371.
29. **Kuner, R., et al.** 2003. TorsinA protects against oxidative stress in COS-1 and PC12 cells. Neurosci. Lett. **350:**153–156.
30. **Leach, N., et al.** 2007. Emerin is hyperphosphorylated and redistributed in herpes simplex virus type 1-infected cells in a manner dependent on both UL34 and US3. J. Virol. **81:**10792–10803.
31. **Loret, S., G. Guay, and R. Lippe.** 2008. Comprehensive characterization of extracellular herpes simplex virus type 1 virions. J. Virol. **82:**8605–8618.
32. **Martin, J. N., T. B. Bair, N. Bode, W. T. Dauer, and P. Gonzalez-Alegre.** 2009. Transcriptional and proteomic profiling in a cellular model of DYT1 dystonia. Neuroscience **164:**563–572.
33. **McLean, P. J., et al.** 2002. TorsinA and heat shock proteins act as molecular chaperones: suppression of alpha-synuclein aggregation. J. Neurochem. **83:**846–854.
34. **Mettenleiter, T. C., B. G. Klupp, and H. Granzow.** 2009. Herpesvirus assembly: an update. Virus Res. **143:**222–234.
35. **Monier, K., J. C. Armas, S. Etteldorf, P. Ghazal, and K. F. Sullivan.** 2000.

Annexation of the interchromosomal space during viral infection. Nat. Cell Biol. **2:**661–665.
36. **Morris, J. B., H. Hofemeister, and P. O'Hare.** 2007. Herpes simplex virus infection induces phosphorylation and delocalization of emerin, a key inner nuclear membrane protein. J. Virol. **81:**4429–4437.
37. **Mou, F., T. Forest, and J. D. Baines.** 2007. US3 of herpes simplex virus type 1 encodes a promiscuous protein kinase that phosphorylates and alters localization of lamin A/C in infected cells. J. Virol. **81:**6459–6470.
38. **Mou, F., E. Wills, and J. D. Baines.** 2009. Phosphorylation of the U_L31 protein of herpes simplex virus 1 by the U_S3-encoded kinase regulates localization of the nuclear envelopment complex and egress of nucleocapsids. J. Virol. **83:**5181–5191.
39. **Naismith, T. V., J. E. Heuser, X. O. Breakefield, and P. I. Hanson.** 2004. TorsinA in the nuclear envelope. Proc. Natl. Acad. Sci. U. S. A. **101:**7612–7617.
40. **Nery, F. C., et al.** 2008. TorsinA binds the KASH domain of nesprins and participates in linkage between nuclear envelope and cytoskeleton. J. Cell Sci. **121:**3476–3486.
41. **Ozelius, L. J., et al.** 1997. The early-onset torsion dystonia gene (DYT1) encodes an ATP-binding protein. Nat. Genet. **17:**40–48.
42. **Padula, M. E., M. L. Sydnor, and D. W. Wilson.** 2009. Isolation and preliminary characterization of herpes simplex virus 1 primary enveloped virions from the perinuclear space. J. Virol. **83:**4757–4765.
43. **Reynolds, A. E., L. Liang, and J. D. Baines.** 2004. Conformational changes in the nuclear lamina induced by herpes simplex virus type 1 require genes U_L31 and U_L34. J. Virol. **78:**5564–5575.
44. **Reynolds, A. E., et al.** 2001. U_L31 and U_L34 proteins of herpes simplex virus type 1 form a complex that accumulates at the nuclear rim and is required for envelopment of nucleocapsids. J. Virol. **75:**8803–8817.
45. **Reynolds, A. E., E. G. Wills, R. J. Roller, B. J. Ryckman, and J. D. Baines.** 2002. Ultrastructural localization of the herpes simplex virus type 1 UL31, UL34, and US3 proteins suggests specific roles in primary envelopment and egress of nucleocapsids. J. Virol. **76:**8939–8952.
46. **Roller, R. J., S. L. Bjerke, A. C. Haugo, and S. Hanson.** 2010. Analysis of a charge cluster mutation of herpes simplex virus type 1 UL34 and its extragenic suppressor suggests a novel interaction between pUL34 and pUL31 that is necessary for membrane curvature around capsids. J. Virol. **84:**3921–3934.
47. **Roller, R. J., and B. Roizman.** 1992. The herpes simplex virus 1 RNA binding protein US11 is a virion component and associates with ribosomal 60S subunits. J. Virol. **66:**3624–3632.
48. **Roller, R. J., Y. Zhou, R. Schnetzer, J. Ferguson, and D. DeSalvo.** 2000. Herpes simplex virus type 1 U_L34 gene product is required for viral envelopment. J. Virol. **74:**117–129.
49. **Ryckman, B. J., and R. J. Roller.** 2004. Herpes simplex virus type 1 primary envelopment: UL34 protein modification and the US3-UL34 catalytic relationship. J. Virol. **78:**399–412.
50. **Scott, E. S., and P. O'Hare.** 2001. Fate of the inner nuclear membrane protein lamin B receptor and nuclear lamins in herpes simplex virus type 1 infection. J. Virol. **75:**8818–8830.
51. **Shashidharan, P., et al.** 2004. Overexpression of torsinA in PC12 cells protects against toxicity. J. Neurochem. **88:**1019–1025.
52. **Shiba, C., et al.** 2000. The UL34 gene product of herpes simplex virus type 2 is a tail-anchored type II membrane protein that is significant for virus envelopment. J. Gen. Virol. **81:**2397–2405.
53. **Simpson-Holley, M., J. Baines, R. Roller, and D. M. Knipe.** 2004. Herpes simplex virus 1 U_L31 and U_L34 gene products promote the late maturation of viral replication compartments to the nuclear periphery. J. Virol. **78:**5591–5600.
54. **Simpson-Holley, M., R. C. Colgrove, G. Nalepa, J. W. Harper, and D. M. Knipe.** 2005. Identification and functional evaluation of cellular and viral factors involved in the alteration of nuclear architecture during herpes simplex virus 1 infection. J. Virol. **79:**12840–12851.
55. **Skepper, J. N., A. Whiteley, H. Browne, and A. Minson.** 2001. Herpes simplex virus nucleocapsids mature to progeny virions by an envelopment → deenvelopment → reenvelopment pathway. J. Virol. **75:**5697–5702.
56. **Tanaka, M., H. Kagawa, Y. Yamanashi, T. Sata, and Y. Kawaguchi.** 2003. Construction of an excisable bacterial artificial chromosome containing a full-length infectious clone of herpes simplex virus type 1: viruses reconstituted from the clone exhibit wild-type properties in vitro and in vivo. J. Virol. **77:**1382–1391.
57. **Terano, T., Y. Zhong, S. Toyokuni, H. Hiai, and Y. Yamada.** 2005. Transcriptional control of fetal liver hematopoiesis: dominant negative effect of the overexpression of the LIM domain mutants of LMO2. Exp. Hematol. **33:**641–651.
58. **Torres, G. E., A. L. Sweeney, J. M. Beaulieu, P. Shashidharan, and M. G. Caron.** 2004. Effect of torsinA on membrane proteins reveals a loss of function and a dominant-negative phenotype of the dystonia-associated ΔE-torsinA mutant. Proc. Natl. Acad. Sci. U. S. A. **101:**15650–15655.
59. **Torrisi, M. R., C. Di Lazzaro, A. Pavan, L. Pereira, and G. Campadelli-Fiume.** 1992. Herpes simplex virus envelopment and maturation studied by fracture label. J. Virol. **66:**554–561.
60. **Vander Heyden, A. B., T. V. Naismith, E. L. Snapp, D. Hodzic, and P. I. Hanson.** 2009. LULL1 retargets torsinA to the nuclear envelope revealing an activity that is impaired by the DYT1 dystonia mutation. Mol. Biol. Cell **20:**2661–2672.
61. **Welsh, G. I., et al.** 2007. Rip11 is a Rab11- and AS160-RabGAP-binding protein required for insulin-stimulated glucose uptake in adipocytes. J. Cell Sci. **120:**4197–4208.
62. **White, S. R., and B. Lauring.** 2007. AAA+ ATPases: achieving diversity of function with conserved machinery. Traffic. **8:**1657–1667.
63. **Worman, H. J., C. Ostlund, and Y. Wang.** 2010. Diseases of the nuclear envelope. Cold Spring Harb Perspect. Biol. **2:**a000760.
64. **Yamauchi, Y., et al.** 2001. Herpes simplex virus type 2 UL34 protein requires UL31 protein for its relocation to the internal nuclear membrane in transfected cells. J. Gen. Virol. **82:**1423–1428.
65. **Ye, G. J., K. T. Vaughan, R. B. Vallee, and B. Roizman.** 2000. The herpes simplex virus 1 U(L)34 protein interacts with a cytoplasmic dynein intermediate chain and targets nuclear membrane. J. Virol. **74:**1355–1363.